MAGNETIC DYNAMICS OF NICKEL FILMS WITH A SQUARE STRIPE STRUCTURE UNDER EXCITATION BY ACOUSTIC PULSES

© 2025 A. V. Golov[a,*], L. N. Kotov[a], Ch. Nayak[b]

[a]*Syktyvkar State University, Syktyvkar, Russia*

[b]*Vellore Institute of Technology, Vellore, India*

**e-mail: antongolov@mail.ru*

Received November 15, 2024

Revised December 14, 2024

Accepted December 30, 2024

Abstract. We studied the conditions for magnetization reorientation of nickel nanofilms with a jagged strip structure when acoustic pulses of a Gaussian shape pass through them. The behavior of such films in a constant magnetic field is studied, hysteresis loops are constructed depending on the angle of field application. The modeling was carried out using the MuMax3 software package. The results of the work can be used in the development of modern compact and energy-efficient magnetic recording devices.

Keywords: *ferromagnets, films with a toothed strip structure, acoustic pulses, magnetization reversal*

DOI: 10.31857/S036767652504007e5

INTRODUCTION

In recent decades, the control of the magnetic state of nanoferromagnets and their nonlinear magnetic dynamics has been of great interest both in practical terms in the design of compact and energy-efficient electronics, magnetic recording, and spintronics devices and in the context of fundamental research into the possibilities of creating magnetic memory nanocells of complex configuration for nonvolatile

information storage and processing [1-3]. The development of such a new field in micromagnetism as ultrafast magnetoacoustics has become possible due to the rapid development of nanotechnologies, cheapening and minimization of laser technologies that allow the use of sufficiently powerful femtosecond lasers for point heating of substrates, leading to the propagation of ultrashort acoustic pulses towards the investigated magnetic sample fixed on the same substrate [4, 5]. The elastic deformation in crystals under such an effect can reach very high values, quite close to the plasticity limit of solids [6].

The control of the magnetic state of rather complex ensembles of band structures and nanomagnets by exposing them to bulk acoustic phonons or surface acoustic waves is characterized not only by energy efficiency but also by high switching rates [2, 7]. In this work, using the specialized micromagnetic simulation package MuMax3, with acceleration on a graphics processor [8], we simulate the process of switching of the magnetization vector in ferromagnetic nanostructures of complex shape, namely, in nickel nanofilms with a bandgap structure, when short acoustic pulses pass through them.

GEOMETRY PROBLEMS AND BASIC EQUATIONS

Ultrafast magnetoacoustics is based on the phenomenon of magnetostriction determined by the interaction between elastic and magnetic subsystems of a ferromagnet. Direct and inverse magnetostriction are distinguished. In direct magnetostriction, a change in magnetization leads to a change in the geometric

dimensions of the sample or the appearance of elastic oscillations, while in reverse magnetostriction, on the contrary, a change in the sample dimensions leads to oscillations of the magnetization vector. These effects can be described within the framework of the phenomenological theory of magnetoelasticity [9], which makes a significant contribution to the magnetic energy density, represented in this study by the sum of the following densities:

$$F = F_{zeem} + F_{aniz} + F_{exc} + F_{dd} + F_{me}, \qquad (1)$$

whereF_{zeem} is the Zeeman energy density,F_{aniz} is the magneto-crystallographic anisotropy energy density,F_{exc} is the exchange energy density,F_{dd} is the dipole-dipole interaction energy density,F_{me} is the magnetoelastic energy density. Knowing the dynamics of the free energy density *F*, we can determine the effective magnetic field$\vec{B}_{eff}$ as its functional derivative. The$\vec{B}_{eff}$ field affects the behavior of magnetization in the sample according to the Landau-Lifshitz equation written in the form [10]

$$\frac{\partial \vec{m}}{\partial t} = -\frac{\gamma}{1+\alpha^2}\left(\left[\vec{m} \times \vec{B}_{eff}\right] + \alpha\left[\vec{m} \times \left[\vec{m} \times \vec{B}_{eff}\right]\right]\right), \qquad (2)$$

where α = 0.04 is the dissipation factor for nickel [6],γ is the gyromagnetic ratio,$\vec{m}$ is the unit vector of the sample magnetization.

A thin film of polycrystalline nickel without magnetocrystalline anisotropy ($F_{aniz} = 0$) was taken as a modeling object, which allowed us to evaluate the effect of the complex shape of the film on its magnetic dynamics. In the MuMax3 micromagnetic modeling package, an object of any shape consisting of a finite number of cuboidal cells considered to be single-domain [8] can be specified as a sample. In

the course of modeling, for each cell of the partition, the magnetic dynamics of its magnetization is calculated according to formula (2), taking into account the influence on it of the magnetization of the other cells of the partition, which is determined mainly by the exchangeF_{exc} and dipole-dipoleF_{dd} interactions. The calculation of the latter remains the most resource-intensive operation in micromagnetic modeling, since at each step of modeling the interaction of each single-domain cell with all other cells of the sample is calculated, and the number of such cells can reach several million. To account for the exchange interaction it is sufficient to consider the influence of only the nearest neighbors. For single-domain samples of simple shapes, the dipole-dipole interaction can be replaced by the tensor of demagnetizing factors [10], which greatly simplifies the calculations but is not applicable in our case.

For convenience, the partitioning cells were taken of cubic shape with the size of 5 5×× 5 nm^3, such cells in the case of nickel will always be single-domain [11]. The linear dimensions of the solid film, without cutouts, were taken such that the number of partition cells along each side was a multiple of powers of two, this allows for faster calculations using the fast Fourier transform in the modeling. The film dimensions were 2560× 2560× 40 nm^3, which is equivalent to two million partitioning cells and allows the boundaries of individual magnetic domains formed in the magnetic structure of the film to be delineated with high resolution. To set the shape inhomogeneity, cutouts with depth *h* and width a were created in the film (Fig. *1a*), which were repeated with a step *w= 2a*, i.e. the distance between the cutouts is equal to their width. The depth of the cutout η is the ratio of the depth of the cutout *h* to the film thickness, for a continuous film with no cutouts η = 0%. In this study, a square film with eight cutouts

was considered in the magnetic dynamics calculations. The film lies in the *XY* plane, and the direction of the stripes coincides with the *Y* axis (Fig. *1b*).

The constant magnetic field$\vec{B}$ acts at an angle *φ* to the *Oh* axis and determines the contributionF_{zeem} to the total free energy density (1). The field due to Heisenberg exchange interaction in the MuMax3 package was calculated by the formula

$$\vec{B}_{exc} = 2\frac{A_{ex}}{M_s}\Delta\vec{m}, \qquad (3)$$

where A_{ex}= 9·10$^{(-12)}$) J/m is the exchange constant and M_s=$_0$.4μ$_o$Tl is the saturation magnetization of nickel [6], μ$_o$is the magnetic constant. The components of the effective magnetic field considered above are independent of time. We will induce reorientation of the film magnetization vector by changing the magnetoelastic energy of the system by passing through the film single short acoustic pulses of bell-shaped or Gaussian form with strain magnitude $\varepsilon_{xx}$and duration τ propagating through the film perpendicular to the strips in the direction of the *Ox* axis. The magnetoelastic field in such a case is defined by only one component:

$$B_{me}^{(x)} = -\frac{2b_1}{M_s}\varepsilon_{xx}m_x, \qquad (4)$$

where b_1= 10^{7}J/m^{3}is the first magnetoelastic constant for nickel [6]. For simplicity, we will assume that the acoustic pulse acts on the whole film simultaneously. Such pulses can be realized by heating the substrate with a femtosecond laser pulse, causing the propagation of surface acoustic waves that then pass through the ferromagnetic film under study, fixed on this substrate [6, 7].

DESCRIPTION OF THE OBTAINED RESULTS ON THE HYSTERESIS LOOP

We consider the behavior of nickel striped films in an external magnetic field in the absence of acoustic influence. By smoothly varying the magnitude of the external magnetic field $\vec{B}$, we constructed hysteresis loops for the normalized film magnetization $\vec{m}$, where the unit value corresponds to the maximum magnetization of the film in one direction, not necessarily coinciding with the direction of the external magnetic field (Fig. 2). Fig. *2a* shows a series of hysteresis loops for films with cutout depth η = 50%, i.e., the cutouts reach the middle of the film, as a function of the angle φ of the external field application, where the angle φ = 0° corresponds to a magnetic field perpendicular to the strips, and 90° corresponds to a parallel magnetic field. The largest hysteresis loop area and the largest coercivity of the film are observed, as expected, at the field $\vec{B}$, applied perpendicular to the strips (φ = 0°). Only in this case, out of all the considered ones, the loop has a gentle shape, i.e., when the field is reduced, such a film transitions from the saturation state to the multidomain state; for the other cases, the residual magnetization is close to unity, which indicates the single-domain state of the film when its magnetization vector is co-directed with the stripes. When the magnetic field is rotated by an angle φ = 30° to the *Oh* axis, the coercivity of the film decreases and takes a minimum value. The magnetization of the film changes by a jump from one metastable position directed along the strips to the opposite one at a critical field value of 5 mTl. Also for this loop, small deviations from saturation magnetization are observed for fields in the range from 9 to 23 mTl, due to the smooth transition of magnetization from stable position along the direction of the strips to the direction coinciding with the direction of the field, with the growth of the

field value. The stable positions of magnetization along the strips can be used as a binary cell of nonvolatile memory.

Similar in shape hysteresis loops are observed for the other cases of the angle φ = 45-90°, the value of the critical reorientation field slowly increases when the angle φ increases from 45° to 60°, and then slightly decreases when approaching the angle of 90°. The most effective from the point of view of minimizing the energy consumption for maintaining a constant magnetic field to simplify the film remagnetization processes will be the application of this field at an angle of 30° to the *Ox* axis, which corresponds to an angle of 60° relative to the film strips.

The hysteresis loops for the magnetic field directed perpendicular to the strips (φ = 0°) at different cutout depths *h* were also plotted (Fig. *2b*). The highest coercive force in this case belongs to the film in which the depth of the notches reaches the middle of the thickness, i.e., this is the most difficult film geometry for its remagnetization. The simplest film geometry is the remagnetization of individual strips when there are no bridges between the strips, i.e., the case of η = 100%. The slight asymmetry of the hysteresis loops for the chosen symmetric film structure is explained by the fact that at the initial moment of time in the absence of a constant magnetic field, the film magnetization vector was directed along the *Oy* axis. Thus, by selecting the angle of magnetic field application and the depth of the film cutout, we can select the optimal value of the critical reorientation field of magnetization in the film, both from the point of view of energy efficiency and from the side of protection against accidental remagnetization of the film.

MAGNETIC DYNAMICS UNDER ACOUSTIC INFLUENCE

Consider the effect of an acoustic pulse on a striped nickel film with a depth of cutout η = 50%, located in a constant magnetic field directed perpendicular to the stripes, i.e., $\varphi = 0°$ and at its value B_x= 10 mTl, which is noticeably less than its critical value of 20 mTl (Fig. 2). In such a case, there are at least two metastable states of the film magnetization configuration, which can be switched by acoustic influence. The farther the field value is from the critical value, the higher the energy barrier that must be overcome to reorient the magnetization by acoustic action [11], but there will be fewer random switches.

We have plotted the time dependences of the behavior of the components of the magnetization vector of the film as a whole under the influence of a Gaussian acoustic pulse with the value $|\varepsilon_{xx}| = 0.45\%$ and duration $\tau = 200$ ps for the cases of film stretching (Fig. *3a*) and compression (Fig. *3b*). In both cases, short magnetization oscillations with a frequency of 7-8 GHz are observed in the film (dashed black line) at the moment of the acoustic pulse passage, but the reorientation of the magnetization vector along the fringe direction or along the *Oy* axis, occurs only at a negative acoustic pulse, i.e., at film compression. Time diagrams of the dynamics of y- and z-components of the total magnetization of the nickel film as a function of the magnitude and duration of the acoustic pulse were also constructed (Fig. *3c-3e*). These diagrams allow us to determine both the presence of reorientation of the magnetization vector in the film and the frequency of oscillations occurring at the moment of the acoustic pulse passage.

Figs. *3c* and *3d* show the influence of the acoustic pulse magnitude with a duration of 200 ps on the behavior of the film magnetization, from the analysis of which

it can be noted that in the whole range of the studied acoustic pulse magnitudes ε_{xx}, no reorientation of the magnetization occurs when the film is stretched, while at compression, i.e., at negative pulses, a whole series of possible final states of the magnetization of cells in the film is observed (Fig. 4). Moreover, the limiting cases of metastable states of the film magnetization along and against the *Oy* axis are separated by tenths of a percent of the acoustic pulse value. An increase in the frequency of oscillation of the magnetization vector with increasing height of the acoustic pulse is observed, both at compression and at stretching of the film (Figs. *3c* and *3d*), which is not observed at changing the pulse duration (Figs. 3d and *3e*). The time diagrams for a pulse with the amplitude ε_{xx} = -0.3%, i.e., with an acoustic impact compressing the film, and a duration from 100 to 500 ps (Figs. *3g* and *3e*) clearly show the influence of the pulse duration on the final position of magnetization. Consequently, controlling the final state of the magnetization vector in the film through the pulse duration seems preferable to controlling it through its amplitude.

As mentioned above, depending on the magnitude and duration of the acoustic pulse, after its passage through the striped film, the portrait of the distribution of the magnetization vectors of the cells varies greatly (Fig. 4), which may be due to the large variation of possible final states for such a large number of cells of the partitioning - about 2 million cells. However, in most cases, the resulting magnetization vector of the whole film was directed along the notches with a tendency to consistency of the magnetization vector directions in neighboring strips.

CONCLUSION

Thus, we have performed micromagnetic modeling of remagnetization processes in nickel nanofilms with striped tooth structure when acoustic pulses of Gaussian shape pass through them using the MuMax3 software package. Hysteresis loops were plotted for different directions of magnetic field application and for different depths of the notch in the films. Time diagrams of film magnetization fluctuations at the moment of acoustic pulse passing into them were also considered. The possibility of switching the magnetization of such toothed striped films by a compressive acoustic pulse is shown, and the control of this transition by adjusting its duration rather than its amplitude looks most promising. The obtained results can be applied and used in the design of modern magnetic recording devices.

FUNDING

The research was supported by a grant from the Russian Science Foundation, project No. 21-72-20048.

REFERENCES

1. *Beaurepaire E., Merle J.C., Daunois A., Bigot J.Y.* // Phys. Rev. Lett. 1996. V. 76. No. 22. P. 4250.

2. *Vlasov V.S., Golov A.V., Kotov L.N. et al.* // Acoust. Phys. 2022. V. 68. No. 1. P. 18.

3. *Iusipova Iu.A., Skidanov V.A.* // Bull. Russ. Acad. Sci. Phys. 2023. V. 87. No. 3. P. 310.

4. *Temnov V.V., Klieber C., Nelson K.A. et al.* // Nature Commun. 2013. V. 4. P. 1468.

5. *Parpiiev T., Hillion A., Vlasov V. et al.* // Phys. Rev. B. 2021. V. 104. No. 22. Art. No. 224426.

6. *Chang C.L., Tamming R.R., Broomhall T.J. et al.* // Phys. Rev. Appl. 2018. V. 10. No. 3. Art. No. 034068.

7. *Yang W.G., Schmidt H.* // Appl. Phys. Lett. 2020. V. 116. No. 21. Art. No. 212401.

8. *Vansteenkiste A., Leliaert J., Dvornik M. et al*. // AIP Advances. 2014. V. 4. No. 10. P. 107133.

9. *Kotov L.N., Dianov M.Yu., Vlasov V.S., Mironov V.V.* // Bull. Russ. Acad. Sci. Phys. 2023. V. 87. No. 4. P. 409.

10. *Coey JMD*. Magnetism and Magnetic Materials. Cambridge University Press, 2010. 313 p.

11. *Golov A.V., Pleshev D.A., Asadullin F.F., et al. //* Chelyabinsk. phys.-Mat. zhurn. 2023. T. 8. № 1. C. 92.

FIGURE CAPTIONS

Fig. 1. Problem geometry, profile (*a*) and film location (*b*).

Fig. 2. Hysteresis loops for the total magnetization of the nickel film as a function of the angle φ of magnetic field application at η = 50% (*a*) and of the cutout value η at φ = 0° (*b*).

Fig. 3. Time dependences of the components of the magnetization vector of the nickel film with the depth of cut η = 50% under the influence of a Gaussian acoustic pulse with the value $|\varepsilon_{xx}| = 0.45\%$ and duration $\tau = 200$ ps when it is in a constant magnetic field $B_x = 10$ mTl (φ = 0°): *a* - compression along the *Ox* axis ($\varepsilon_{(xx)}<_0$), *b* - stretching

along the *Ox* axis ($\varepsilon_{(xx)}>_0$). Time diagrams of the dynamics of the components of the total magnetization of the nickel film with the depth of cut η = 50% at B_x= 10 mTl (φ = 0°) as a function of the magnitude of the Gaussian acoustic pulse (*c*, *e*: τ = 200 ps) and its duration (*d*, *f*: ε_{xx}= -0.3%). The white line in Figures *c*, *e* schematically indicates the shape of the Gaussian pulse with duration τ = 200 ps, and in *d*, *f* - the limits of its duration τ.

Fig. 4. Initial state (*a*) and possible final states (*b*, *c*, *d*) of the cell magnetization in the film for the cutout depth η = 50%.

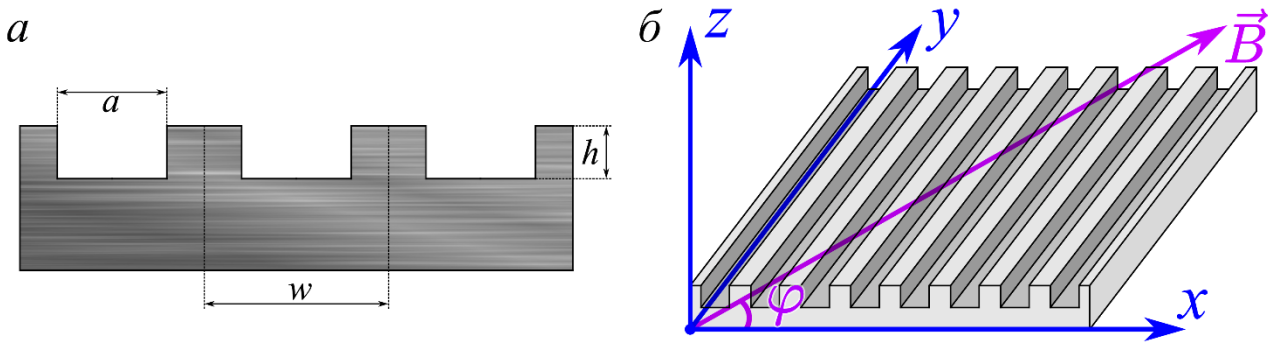

Fig. 1.

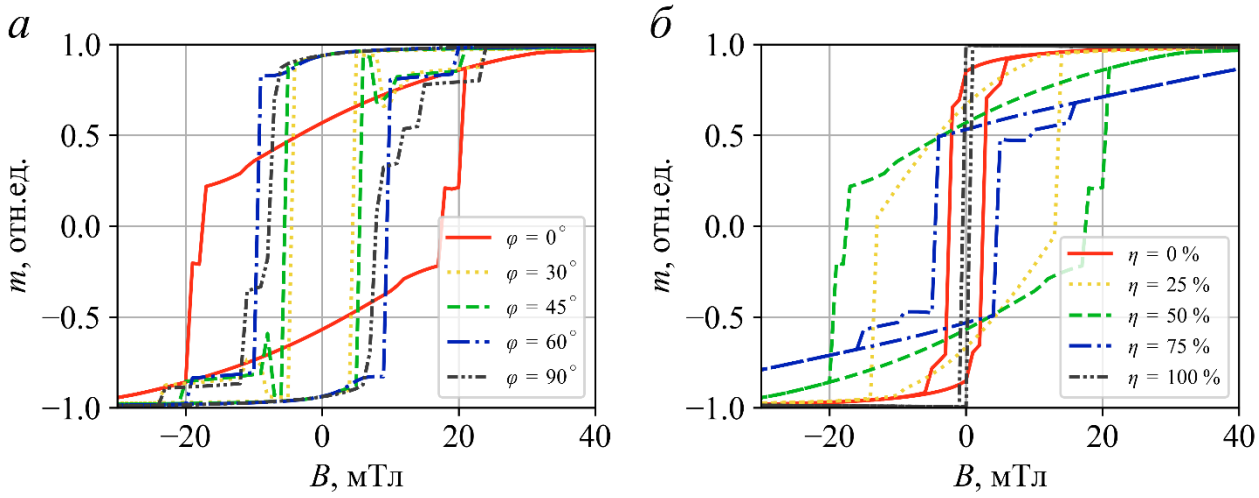

Fig. 2.

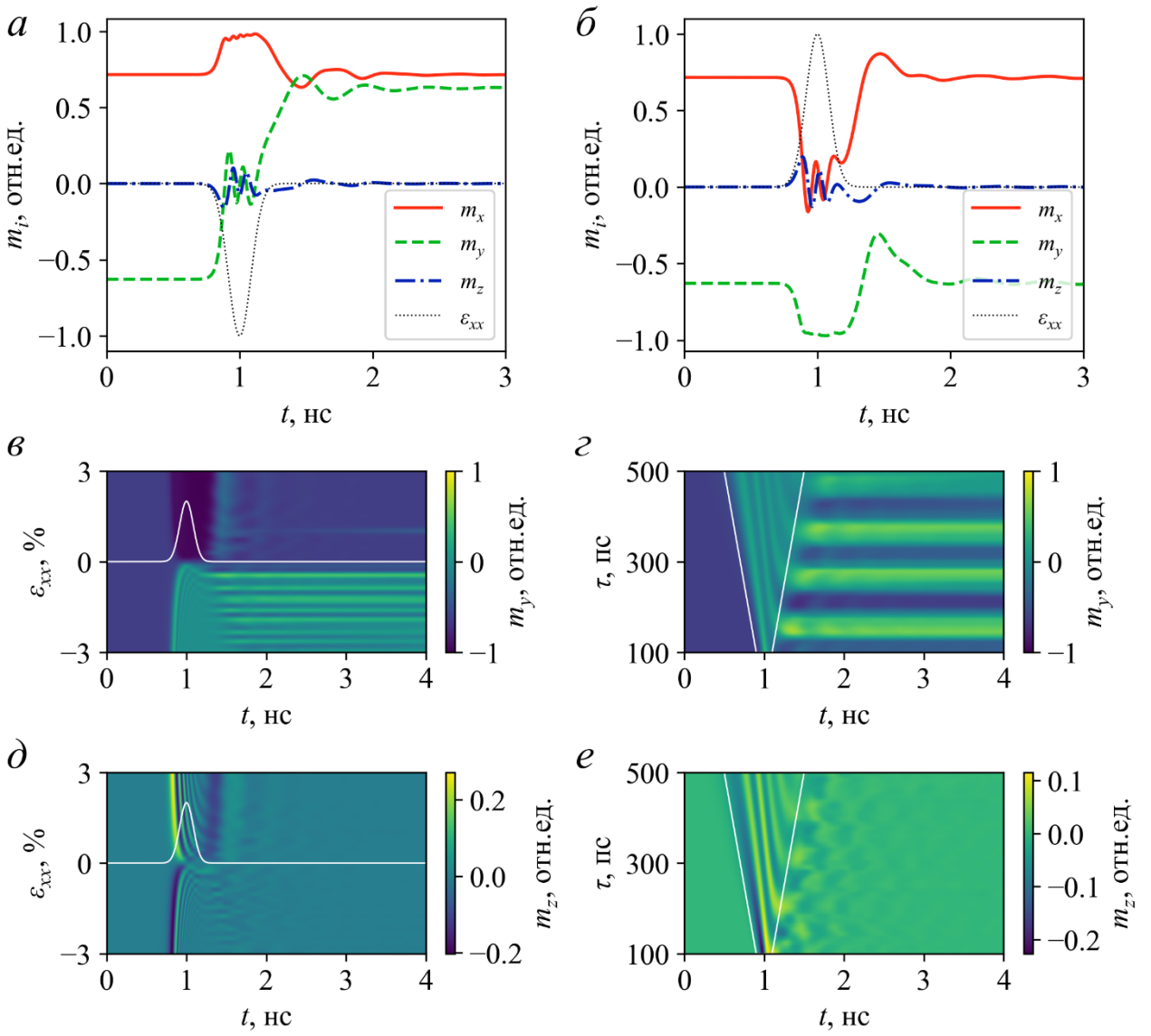
а
б
в
г
д
е
m_i, отн.ед.
t, нс
m_x
m_y
m_z
ε_{xx}
ε_{xx}, %
τ, пс
m_y, отн.ед.
m_z, отн.ед.

Fig. 3.

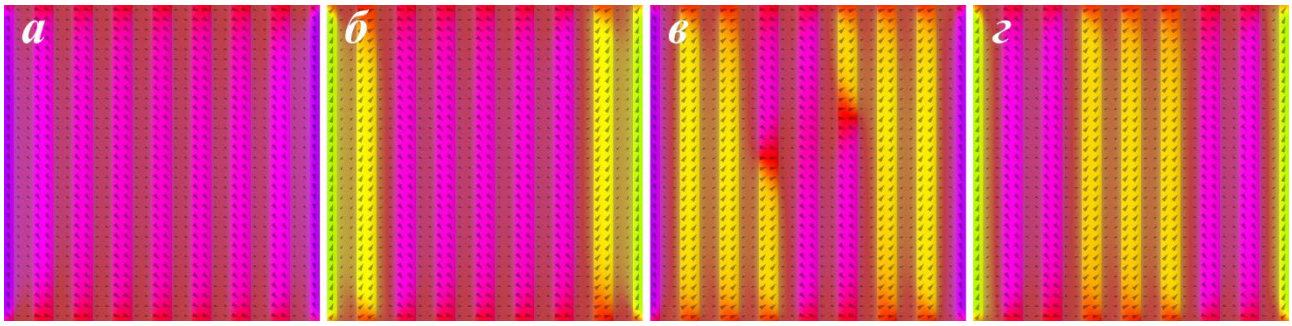
а
б
в
г

Fig. 4.